DOI: 10.1002/adsc.201500171

A Zinc-Dependent Alcohol Dehydrogenase (ADH) from *Thauera aromatica*, Reducing Cyclic α- and β-Diketones

Christoph Loderer,[a] Frances Morgenstern,[a] and Marion Ansorge-Schumacher[a,*]

[a] Chair of Molecular Biotechnology, Institute of Microbiology, Technische Universität Dresden, Zellescher Weg 20b, 01062 Dresden, Germany
Fax: (+49)-351-463-39520; phone: (+49)-351-463-39519; e-mail: marion.ansorge@tu-dresden.de

Received: February 23, 2015; Revised: April 15, 2015; Published online: May 12, 2015

Supporting information for this article is available on the WWW under http://dx.doi.org/10.1002/adsc.201500171.

Abstract: Zinc-dependent alcohol dehydrogenases (ADHs) are valuable biocatalysts for the synthesis of chiral hydroxy compounds such as α-hydroxy ketones and diols, both valuable precursors for the synthesis of various pharmaceuticals. However, while highly active on aliphatic or phenyl-substituted diketones, most well characterized ADHs show no significant activity on cyclic α- and β-diketones. Therefore, this study aimed at the detection of a novel ADH capable to reduce these special targets. It involved a rational screening of biochemical pathways for enzymes with structurally related natural substrates. The so detected 6-hydroxycyclohex-1-ene-1-carbonyl-CoA dehydrogenase (ThaADH) from *Thauera aromatica* was cloned, expressed in *Escherichia coli* and purified by affinity chromatography. The characterization revealed a substrate specificity with highest activities on cyclic α- and β-diketones including 1,2-cyclohexanedione and 1,3-cyclopentanedione. Structural reasons for this extraordinary substrate spectrum were investigated with a homology model created *via* Swiss Model server. Although the quality of the model may be improved, it suggests that a bulky aromatic residue, that plays a crucial role in the definition of the substrate binding pockets of most ADHs, is replaced by a glycine residue in ThaADH. We propose that this structural difference leads to the formation of one large binding pocket instead of two smaller ones and consequently to a preference for cyclic diketones over linear bulky substrates. Thus, we have achieved both provision of a novel biocatalyst with high potential in chiral synthesis, and a possible explanation for the measured differences to known ADHs. The described structural motif might be used for identification of further enzymes with a related substrate scope.

Keywords: biocatalysis; carbonyl reduction; enzyme catalysis; oxidoreductases

Introduction

Alcohol dehydrogenases (ADHs) are a diverse group of enzymes that catalyze the reversible reduction of carbonyl functions to the corresponding alcohols. Their often high chemo-, regio- and stereoselectively make them potential tools for biocatalytic application. For asymmetric synthesis, zinc-dependent medium chain ADHs have been described as particularly useful. Enzymes in this category are constituted of about 340 amino acids and share the Rossman fold motif containing two zinc atoms per subunit.[1] The first zinc atom is directly involved in catalysis while the second is important for the overall structure of the enzyme.[2,3]

Zinc-dependent ADHs have been applied in the synthesis of various chiral hydroxy compounds such as aliphatic diols, hydroxy acids, hydroxylated isoprene derivatives and benzyl alcohol derivatives.[4,5,6,7] A very interesting class of products are α-hydroxy ketones that can be obtained either by selective oxidation of a chiral diol or reduction of a prochiral diketone.[8] A number of ADHs were already demonstrated to efficiently catalyze the reduction of linear aliphatic diketones such as 2,3-pentanedione, to the corresponding hydroxy ketone.[9,10,11,12] Substrate specificity and stereoselectivity in these reactions are described by a widely accepted molecular model in which the two substituents of the carbonyl function are fitted into a small and a large alkyl site within the enzyme, respectively, defining the orientation of the substrate in the active site.[13,14,15] In contrast, little information exists on ADH-catalyzed conversion of cyclic diketones. Most common ADHs were either

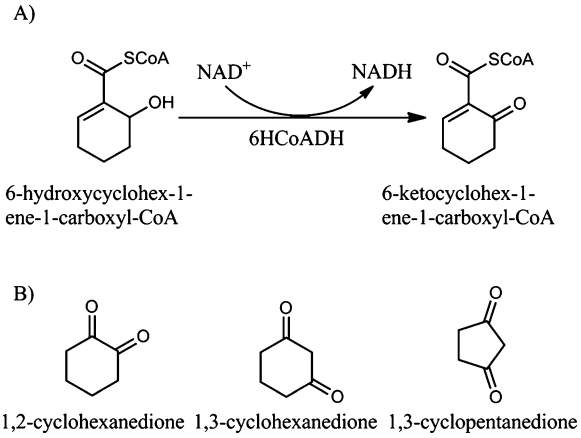

Figure 1. A) Physiological reaction of 6-hydroxycyclohex-1-ene-1-carbonyl-CoA dehydrogenase (6HCoADH) in the benzoate degradation pathway.[22] B) Target substrates for enzymatic reduction.

not tested or determined to be not active towards these substrates.[10,11,12,16] A few reports describe reduction of 1,2-cyclohexanedione, 1,3-cyclohexanedione and 1,3-cyclopentanedione (Figure 1B), which were used as model compounds in this study. A non-identified NADPH-dependent enzyme from yeast was shown to reduce 1,2-cyclohexanedione with decent activities.[17] As well, ADHT from *Thermoanaerobacter ethanolicus* 39E converted 1,2-cyclohexanedione, but only with 5% of the reaction rate, revealed on its best substrate.[18] A not further specified carbonyl reductase KRED101 from Merck was shown to be able to catalyze the reduction of 4,4-dimethoxytetrahydro-2*H*-pyran-3-one, which is structurally related to the described model substrates.[19,20] The NADPH-dependent 3-hydroxycyclohexanone dehydrogenase from a denitrifying *Pseudomonas* species exhibits good activities for the oxidation of cyclic diols but only very low relative activities for the reduction of 1,2-cyclohexanedione and 1,3-cyclohexanedione (3% each).[21]

In conclusion, no well characterized ADH is available to date that is able to reduce cyclic diketones such as 1,2-cyclohexanedione and 1,3-cyclohexanedione with acceptable reaction rates. Consequently, this study aimed for the detection, provision and characterization of a novel ADH to fill this gap. Homology modeling was used to identify structural differences between the novel enzyme and well-established reference ADHs such as carbonyl reductase from *Candida parapsilosis* (CPCR2) and thus provide an explanation for the differences in substrate specificities.

Results and Discussion

Screening of Metabolic Pathways

In order to identify ADHs with a probable capability for reduction of cyclic diketone compounds, metabolic pathways were scanned on the KEGG metabolic pathway database. Metabolic steps with carbonyl reduction or alcohol oxidation reactions on natural substrates with a structural similarity to 1,2-cyclohexanedione and 1,3-cyclohexanedione were screened. Six promising reactions involved in different metabolic pathways were detected. Where available, enzymes proposed or described to catalyze these reactions were assigned to their protein families by applying the Pfam database. This assignment yielded one promising alcohol oxidation being catalyzed by mainly-zinc-dependent ADHs. It is part of the bacterial degradation of benzoate and involved oxidation of 6-hydroxycyclohex-1-ene-1-carboxyl-CoA to 6-oxocyclohex-1-ene-1-carboxyl-CoA (Figure 1A) by a 6-hydroxycyclohex-1-ene-1-carbonyl-CoA dehydrogenase (6HCoADH, EC 1.1.1.368).[22] In the product 6-oxocyclohex-1-ene-1-carbonyl-CoA, the carbon atom in the α-position to the reactive hydroxy function is sp^2-hybridized as is the case in 1,2-cyclohexanedione (Figure 1B). Instead of a second carbonyl group an extremely bulky CoA-thio ester group is present which suggests that, from a sterical point of view, 1,2-cyclohexanedione should also fit in the active site. 6HCoADH was therefore a promising candidate for the reduction of the model cyclic diketones.

The benzoate degradation pathway is mainly found in proteobacteria such as *Thauera*, *Geobacter* and *Rhodopseudomonas* species with 6HCoADH being described as a characteristic enzyme.[23] Its physiological role has been demonstrated for the enzyme from *Thauera aromatica* which was cloned and recombinantly expressed in *E. coli* for this purpose. The enzyme was described as a homo dimer with a molecular weight of 38 kDa per subunit[24] and shown to accept NAD^+, but not $NADP^+$ as cofactor. It formed the basis of all the following experiments and for simplicity was renamed ThaADH.

Provision of ThaADH

The ThaADH gene obtained from *Thauera aromatica* genomic DNA was fused to a DNA-sequence coding for a C-terminally attached StrepTagII to facilitate protein purification and identification, and was expressed in *E. coli* BL21(DE3). Expression resulted in a protein with a molecular weight of about 40 kDa (Figure 2A), which was predominantly in the soluble protein fraction of the cell lysate (Figure 2B). The identity of the ThaADH-StrepTagII fusion protein

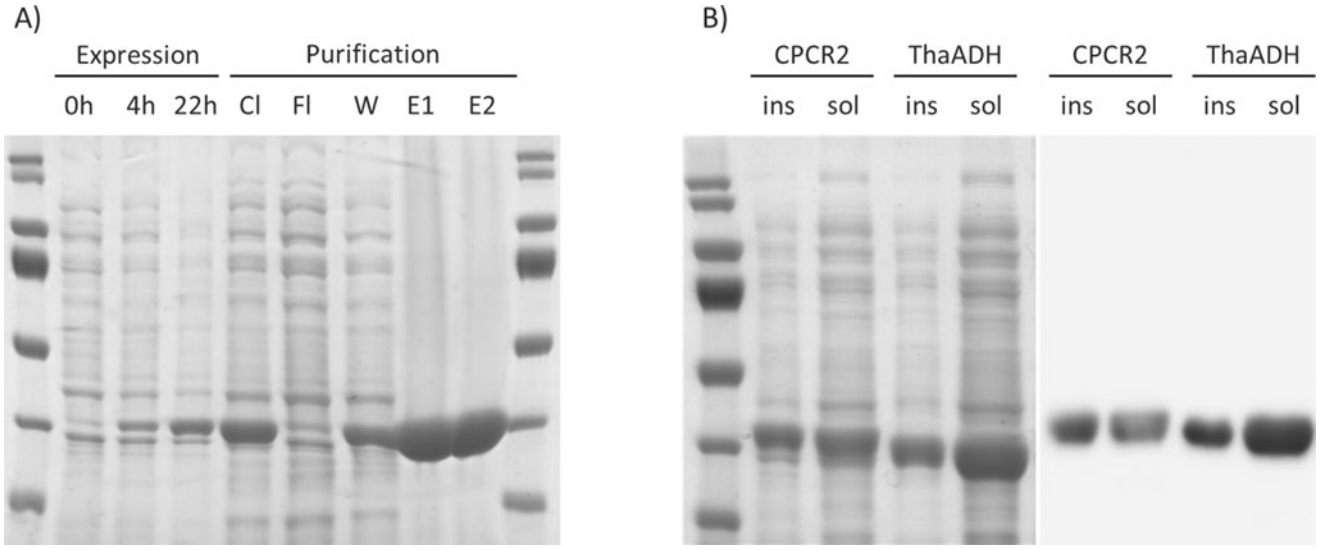

Figure 2. A) Coomassie stained SDS-PAGE of the ThaADH after recombinant expression in *E. coli* and after purification, respectively. Cl: cleared lysate, Fl: column flowthrough, W: washing fraction, E1: elution fraction 1, E2: elution fraction 2. B) Coomassie stained SDS-PAGE and immunodetection of StrepTagII in the insoluble (ins) and soluble (sol) fraction of *E. coli* lysate after ThaADH-expression. Strep-tagged CPCR2 was used as a positive control.

was confirmed *via* Anti-StrepTagII Western blot (Figure 2B). After purification, no major impurities (Figure 2A) were observed. The total protein yield was 22 mg from 400 mL culture volume.

Reactivity of ThaADH

The substrate spectrum of ThaADH with regard to carbonyl reduction was measured for various aldehydes, ketones and especially diketones (Figure 3). Interestingly, ThaADH converts neither acetophenone nor benzaldehyde which are both preferred substrates of many known zinc-dependent ADHs, such as CPCR2 from *Candida parapsilosis*, SsADH from *Sulfolobus solfataricus*, TADH from *Thermus* sp., ADH-A from *Rhodococcus ruber* and HlADH from horse liver.[10,12,16,25,26] Moreover, the enzyme actually prefers substrates with the reactive carbonyl function being located inside a cyclohexyl or cyclopentyl structure. With 0.14 $U \cdot mg^{-1}$ the highest specific activity was measured for 1,2-cyclohexanedione, which is in accordance with the highest structural similarity of this compound to the natural substrate, 6-hydroxycyclohex-1-ene-1-carbonyl-CoA. 1,3-Cyclohexanedione is converted four-fold slower and 1,4-cyclohexanedione is not accepted at all. The specific activity for unsubstituted cyclohexanone is 0.10 $U \cdot mg^{-1}$ and therefore lower than for the *ortho*-substituted 1,2-cyclohexanedione. Hence, *ortho*-substitution of the reactive carbonyl group is obviously beneficial, *meta*-substitution is accepted and *para*-substitution is detrimental for the reductive activity of ThaADH. Summarizing these observations we could show that ThaADH exhibits its highest catalytic activities on compounds similar to its natural substrate. Hence the prediction that an enzyme with structurally related natural substrates should be able to reduce the model compounds was confirmed.

Since 1,2-cyclohexanedione yielded the highest reaction velocities it was applied for the measurements of pH and temperature dependences of ThaADH. The pH profile shows a sharp pH optimum for the reduction reaction at 6.0 with a residual activity of 40% at pH 7.0 (Figure 4A). For acidic pH the activity decrease is even stronger. Concerning temperature the highest activity was measured at 50 °C (Figure 4B). Higher temperatures lead to a very fast precipitation of the enzyme disturbing the photometrical measurement.

Dependency of enzyme activity on substrate concentration was determined for different substrates. For 2,3-pentanedione, a nearly linear increase in enzyme activity was measured up to 200 $mmol \cdot L^{-1}$ indicating a K_M value >100 $mmol \cdot L^{-1}$. In the case of cyclohexanone and 1,2-cyclohexanedione K_M could be more exactly determined yielding 12.1 and 9.3 $mmol \cdot L^{-1}$, respectively (Figure 4C). Thus, despite the lack of exact information for 2,3-pentanedione, it is obvious that ThaADH shows a significantly higher affinity to both cyclic carbonyl substrates. With 5.1 $U \cdot mg^{-1}$ the maximal specific activity for reduction of 1,2-cyclohexanedione is only 50% lower than for the natural substrate (11.8 $U \cdot mg^{-1}$).[24] In contrast, K_M for oxidation of 1,2-cyclohexanedione is 150-fold higher than for reaction on the natural substrate (60 $\mu mol \cdot L^{-1}$). However, although the affinity to the cyclic diketone is lower compared to the natural sub-

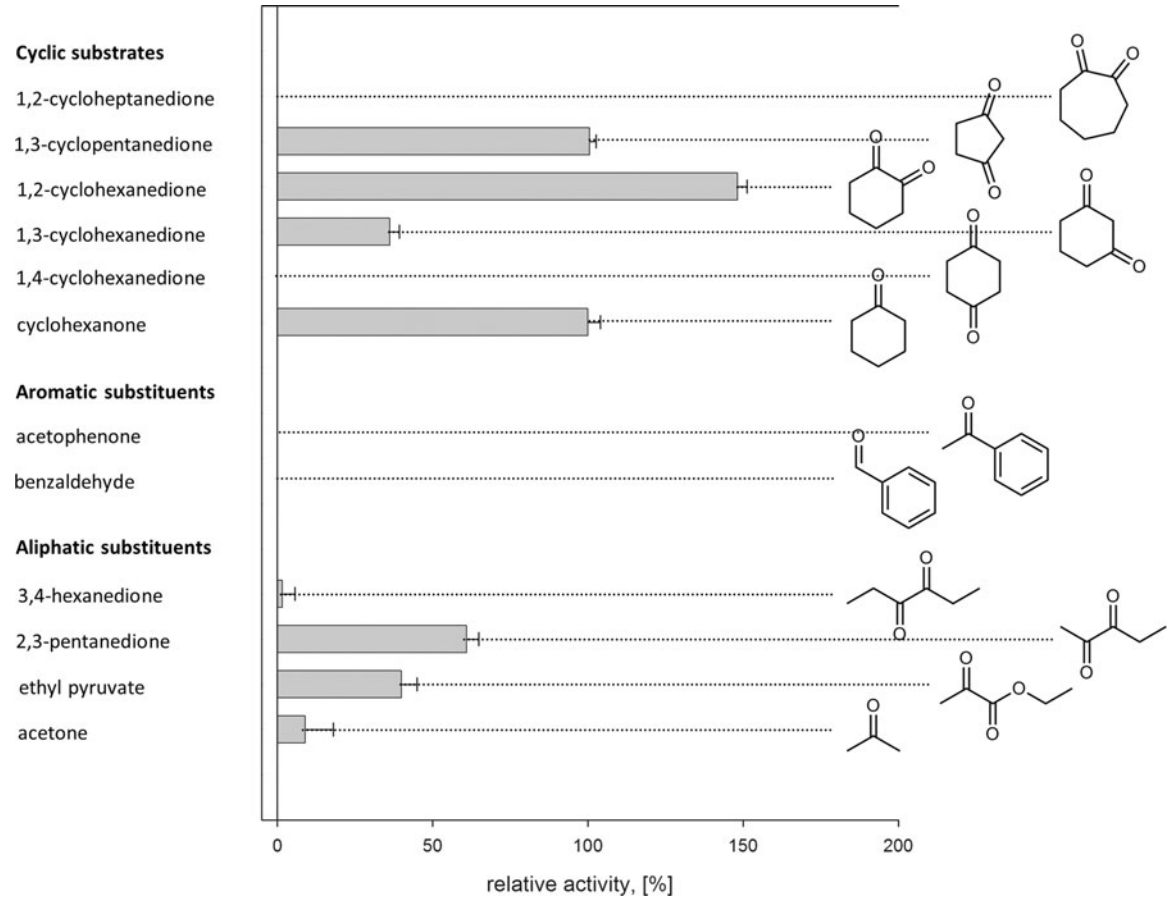

Figure 3. Substrate specificity of ThaADH. *Assay conditions:* buffer: triethanolamine (pH 6.4, 100 mmol·L^{-1}), $T = 50$ °C, substrate (3 mmol·L^{-1}), NADH (250 μmol·L^{-1}), ThaADH (100 μg·mL^{-1}). All measurements were conducted in triplicate.

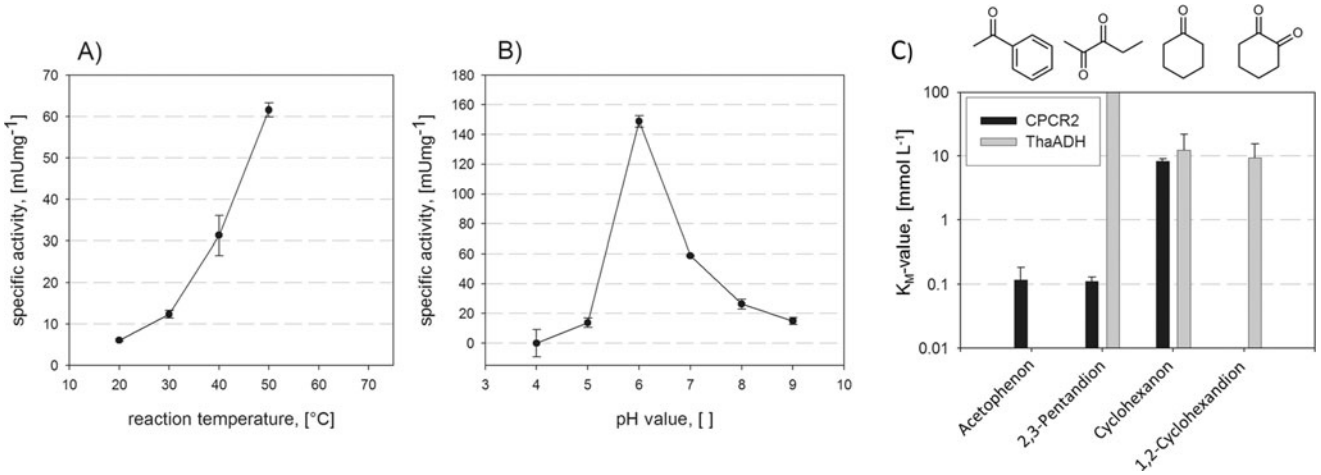

Figure 4. A) pH-dependent activity profile of ThaADH. *Assay conditions:* buffers: pH 4.0, 5.0: acetate (100 mmol·L^{-1}), pH 6.0: phosphate (100 mmol·L^{-1}), pH 7.0, 8.0, 9.0 triethanolamine (TEA) (100 mmol·L^{-1}), $T = 50$ °C, 1,2-cyclohexanedione (3 mmol·L^{-1}), NADH (250 μmol·L^{-1}), ThaADH (100 μg·mL^{-1}). B) Temperature-dependent activity profile of ThaADH. *Assay conditions:* buffer: TEA (pH 6.4, 100 mmol·L^{-1}), $T = 50$ °C, 1,2-cyclohexanedione (3 mmol·L^{-1}), NADH (250 μmol·L^{-1}), ThaADH (100 μg·mL^{-1}). C) Kinetic parameters of ThaADH and CPCR2 for the reduction of carbonyl compounds.

strate, it is higher than for the best linear diketone. This again confirms the preference of ThaADH for cyclic diketones.

The reaction products of 1,2-cyclohexanedione reduction were identified *via* GC-MS. Thereby 2-hydroxy-cyclohexanone was identified as sole reaction

product (Supporting Information, Figures S2–S6), whereas the corresponding diol was not detected. This indicates a specific mono-reduction of the diketone substrate by ThaADH.

Structural Determinants of ThaADH Activity

The amino acid sequence of ThaADH shows a significant similarity to the well described ADHs such as CPCR2 (47%) and ADH 'A' (44%). Despite these sequence similarities the substrate spectrum of ThaADH clearly shows that the active site of the enzyme should possess a significantly different structure in comparison to the ADHs described before. Since a crystal structure of ThaADH is not available, homology models of the enzyme were created to elucidate this matter. The best models obtained *via* the Swiss model homology modeling server were based on cod liver class I alcohol dehydrogenase (1cdo.1.B) and an ADH from *Bacillus stearothermophilus* (1rjw.1.A), respectively, as templates.[27,28] Unfortunately, the overall quality of the models is quite poor due to the only low sequence identities between ThaADH and the template enzymes (33% and 34%, respectively). This is indicated by the low GMQE value (Table 1), which describes the expected accuracy of the model with a maximum value of 1. On the other hand, the two models derived from completely different templates are in good agreement (Figure 5A). To check whether the homology model is appropriate to describe the active site, the local quality (IDDT) of the model was reviewed for each residue. The regions with lowest local quality were identified as loops, located on the protein surface, and as parts of the subunit interface. In contrast, the active site residues, which are located in a cleft, exhibit a significantly better quality than the overall model (Table 1).

Table 1. Parameters and scores of the ThaADH homology models based on the templates cod liver class I alcohol dehydrogenase (1cdo.1.B) and ADH from *Bacillus stearothermophilus* (1rjw.1.A).

Model	Template		Model quality	
	PDB file	Sequence similarity	GMQE[a]	IDDT Average[b]
1	1cdo.1.B	0.33	0.6	0.74
2	1rjw.1.A	0.34	0.6	0.69

[a] GMQE: expected accuracy of the homology model;[33,34] IDDT: expected local similarity to the target;[33,34]
[b] IDDT average: average IDDT values from six active site residues (MM).

The derived models were compared to the available crystal structure of CPCR2 from *Candida parapsilosis*, ADH-A from *Rhodococcus ruber*, SsADH from

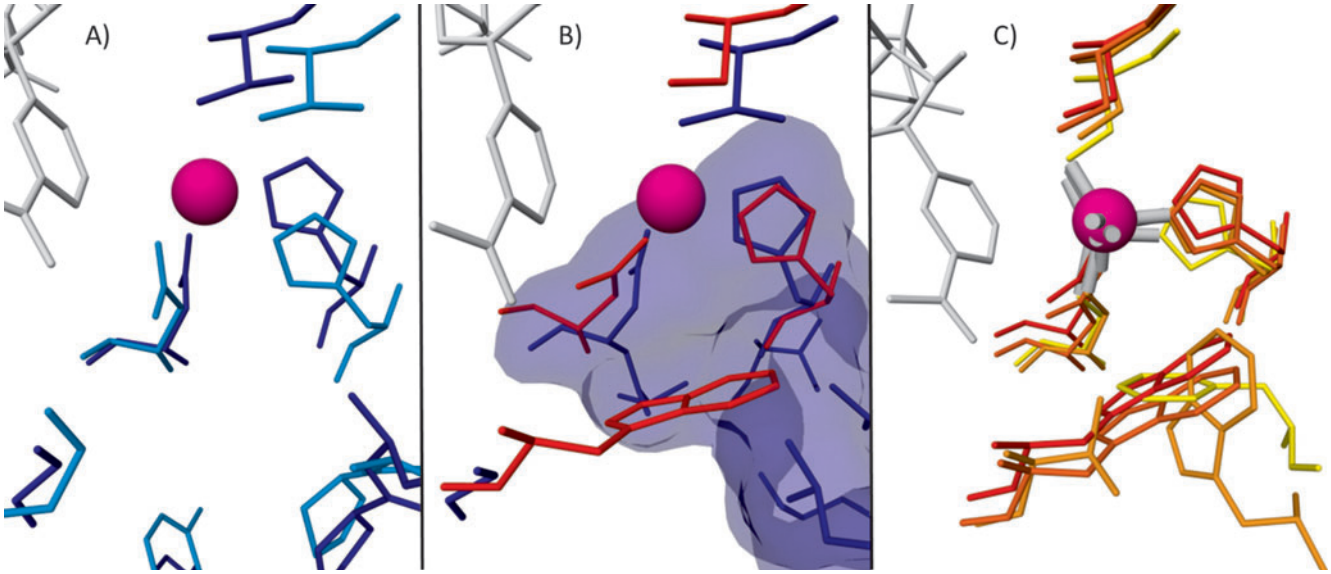

Figure 5. A) Superposition of the two homology models of ThaADH based on the known crystal structures of cod liver class I alcohol dehydrogenase (1cdo.1.B, dark blue) and an ADH from *Bacillus stearothermophilus* (1rjw.1.A, bright blue), respectively, as template. B) Superposition of the homology model of ThaADH based on cod liver class I alcohol dehydrogenase and known crystal structure of CPCR2. Highlighted are the catalytic zinc atom (magenta), the cofactor NADH (grey) as well as G316 in ThaADH (blue) and W286 in CPCR2 (red). The surface of ThaADH residues in the relevant part of the active site is shown in blue. C) Superposition of the crystal structures of the zinc-dependent ADHs CPCR2 (red), SsADH from *Sulfolobus solfataricus* (bright orange), ADH-A from *Rhodococcus ruber* (dark orange) and HlADH from horse liver (yellow). Highlighted are the catalytic zinc atom (magenta), the cofactor NADH (grey) and the aromatic amino acid corresponding to W286 in CPCR2 (red).

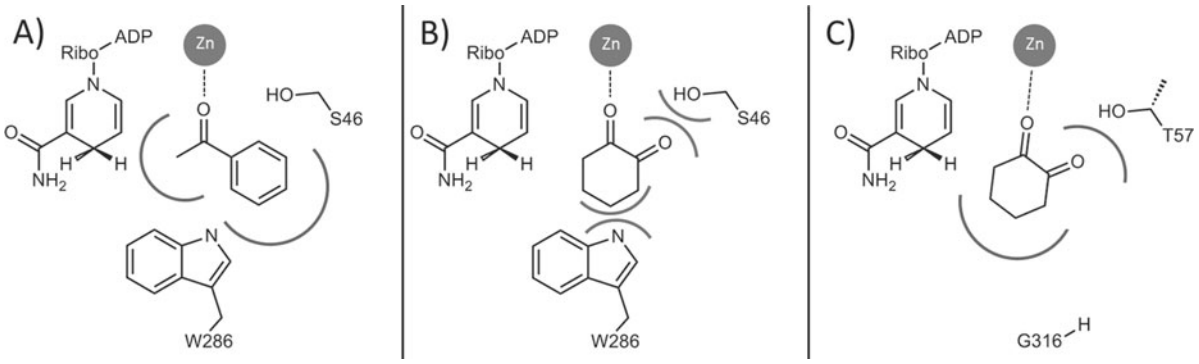

Figure 6. Schematic model of the proposed function of residue G316 in ThaADH and the corresponding residue W286 in CPCR2. A) Catalytically active binding of acetophenone in CPCR2. B) Possible clashes in a potential non-productive binding of 1,2-cyclohexanedione in CPCR2. C) Catalytically active binding of 1,2-cyclohexanedione in ThaADH.

Sulfolobus solfataricus and HlADH from horse liver.[29,30,31,32] In Figure 5B, the superposition of the monomeric structures of CPCR2 and ThaADH is shown. The superposition yielded a RMSD of 1.407 Å over 301 residues, confirming the expected structural similarity. ThaADH residues C55, H78 and D169 align with the CPCR2 residues C44, H65 and D154 coordinating the catalytic zinc residue. ThaADH residue T57 aligns with S46 in CPCR2, which acts as proton donor during the reduction reaction (Figure 5B).

Comparison of the neighboring residues constituting the active site of the different enzymes reveals one major structural difference. W286 which is restricting the active site of CPCR2 in a distance of 5.3 Å to the catalytic zinc atom is exchanged for a glycine (G316) in ThaADH. A bulky aromatic residue at this position is structurally conserved amongst all reference ADHs and was described to be a constituent of the small substrate binding pocket on the boundary to the large one (Figure 5C).[29] Thus, it could act as a wedge separating the two substrate binding pockets, but could also limit the available space for cyclic substrates. Assuming the homology model is accurate the removal of this wedge results in the formation of one large hydrophobic binding pocket improving access of cyclic substrates to the active site.

Based on this observation and the measured kinetic parameters we propose the following model for the impact of the structural difference between ThaADH and CPCR2 in positions G316 and W286: When the high affinity substrate acetophenone binds to CPCR2, the small methyl and the large phenyl substituent of the substrate are located in the small and the large alkyl sites, respectively (Figure 6A).

The alkyl sites are separated by W286. In a comparable binding position, the ring structure of cyclic substrates may clash with the residue separating the alkyl sites (Figure 6B). In case of comparably flexible ring structures such as cyclohexanone, binding is still possible due to a conformational adaption of the substrate,[35] illustrated by the high, but detectable K_M value (Figure 4C). For inflexible cyclic substrates such as 1,2-cyclohexanedione no catalytically active binding is possible due to potential clashes with W286 or other active site residues such as S46. In ThaADH the presence of a glycine residue in the corresponding position leads to the formation of one large binding pocket. Thus, even the sterically inflexible 1,2-cyclohexanedione can be bound in a catalytically active position (Figure 6C) with a K_M value of 9.3 mmol·L^{-1}. In turn, the absence of two distinct binding pockets for the substituents of linear substrates leads to a reduced affinity for this type of compounds, as measured for 2,3-pentanedione. Unfortunately, replacement of W286 in CPCR2 by another amino acid does not yield active variants.

This was observed during site saturation of this residue in a previous study (detailed data will be published elsewhere). The physical replacement of tryptophan in the active site most likely resulted in a severe destabilization, preventing an observable phenotype. Thus, a direct proof for the hypothesized effect of a W286 analogue missing in ThaADH has still to be delivered.

Conclusions

It was demonstrated in this study that data mining in metabolic pathways based on structural similarities of substrates and defined reaction types is an appropriate tool for identification of biocatalysts with novel specificities. Accordingly, a novel zinc-dependent ADH, with a preference for mono-reduction of sterically demanding cyclic diketones was identified. Supported by homology modeling and kinetic parameters, an exchange of a bulky aromatic residue to glycine in the active site of this enzyme can be proposed to play a crucial role for its extraordinary substrate specifici-

ty. However, due to the potential inaccuracy of the homology model, a crystal structure will be necessary to proof this postulation.

Due to its exceptional substrate specificity ThaADH has a high potential for a biocatalytic application in the reduction of diketones. In addition, this enzyme may be used as a starting point in the search for further biocatalysts accepting sterically demanding diketone substrates. A further structural investigation of ThaADH will also be of great value for the elucidation of structural determinants in the substrate specificity of ADHs in general.

Experimental Section

General Information

If not stated differently, all chemicals and oligonucleotides were purchased from Sigma–Aldrich (Sigma–Aldrich, St. Louis, MO, USA), media components were purchased from Carl Roth (Carl Roth GmbH & Ko. KG, Karlsruhe, Germany) and enzymes for molecular cloning were purchased from Thermo Scientific (Thermo Fisher Scientific inc, Waltham, MA, USA).

Cloning of the thaADH Gene

The thaADH gene (Genbank GI: 19571180) was obtained *via* PCR from genomic DNA from *Thauera aromatica* provided by Leibniz-Institut DSMZ (Deutsche Sammlung von Mikroorganismen und Zellkulturen GmbH, Braunschweig, Germany). The PCR was conducted with Phusion® High-Fidelity DNA Polymerase (Thermo Fisher Scientific, Waltham, MA, USA) according to the manufacturer's instructions. The primers *Thauera* NdeI for: `cattcatATGGCGGCGAAGAGTTC` and *Thauera*_HindIII_rev: `gtataagcttGGGCGTGAGGATGG` were applied introducing a NdeI and a HindIII restriction site in the PCR product. With these restriction sites the thaADH gene was ligated into the multiple cloning site of a modified pET22b(+) expression vector under the control of a T7 promoter. Thereby a linker coding for ten alanine residues followed by a StrepTagII was fused to the C-terminus of the gene. *E.coli* DH5α was transformed with this vector and screened for positive clones *via* colony PCR. For selected positive clones a plasmid preparation was performed followed by sequencing by GATC biotech (GATC Biotech AG, Konstanz, Germany).

Expression of ThaADH-Streptag Fusion Protein

In order to utilize the T7 expression system, the sequenced vector was transformed into *E.coli* BL21(DE3).[36] Induction time, inductor concentration, expression temperature and expression time were optimized. The highest expression was achieved with the following protocol: 400 mL LB medium containing 100 $\mu g \cdot mL^{-1}$ ampicillin were inoculated from an overnight preculture to a final OD_{600} of 0.05 and incubated at 37 °C and 150 rpm in an Infors Minitron shaker (Infors GmbH, Einsbach, Germany) to an OD_{600} of 0.8. Then, expression was induced by addition of 1 $mmol \cdot L^{-1}$ IPTG and the temperature was reduced to 15 °C. The cell were harvested after 22 h by centrifugation (4 °C, 8000 rpm, 10 min) and stored at −20 °C.

Purification of ThaADH-Streptag Fusion Protein

Cell lysis was conducted by a combination of lysozyme digestion and ultrasonification. The cells were first resuspended in cell lysis buffer containing 100 $mmol \cdot L^{-1}$ triethanolamine (TEA), 150 $mmol \cdot L^{-1}$ NaCl, 1 $mmol \cdot L^{-1}$ PMSF, 50 $\mu g \cdot mL^{-1}$ lysozyme and 5 $\mu g \cdot mL^{-1}$ DNAseI (AppliChem GmbH, Darmstadt, Germany). After incubation for 90 min at 6 °C and 2 min of sonification (Sartorius Labsonic M, Settings: Cycle = 0.6, Amplitude = 100%), cell debris were removed by centrifugation (4 °C, 16000 rpm, 30 min).

For protein purification Strep-Tactin® Sepharose® 5 mL gravity flow columns (IBA GmbH, Goettingen, Germany) were utilized. The columns were equilibrated with 25 mL washing buffer (100 $mmol \cdot L^{-1}$ TEA, 150 $mmol \cdot L^{-1}$ NaCl, 1 $mmol \cdot L^{-1}$ EDTA at pH 7.0). The cleared lysate containing ThaADH-streptag fusion protein was applied on the column. After washing with 10 mL of washing buffer, bound protein was released with 15 mL elution buffer (100 $mmol \cdot L^{-1}$ TEA, 150 $mmol \cdot L^{-1}$ NaCl, 2.5 $mmol \cdot L^{-1}$ Desthiobiotin at pH 7.0) in 2 mL fractions. The fractions with the highest activity were pooled. After addition of glycerol to a final concentration of 40% the protein was stored at −20 °C.

CPCR2 was expressed and purified according to the protocol described by Jakoblinnert.[7]

Polyacrylamide Gel Electrophoresis and Western Blot

SDS-PAGE was performed according to the procedure of Lämmli[37] applying the Invitrogen XCell SurelockTM system (Life Technologies, Carlsbad, CA, USA). For the expected 40 kDa target protein a tris-glycine gel containing 12% acrylamide was utilized. Samples were incubated for 10 min at 95 °C in loading buffer and 15 μL were loaded on the gel. In addition 5 μL of PageRuler Prestained Protein Ladder were loaded on the gel. The gel was run for 80 min at 180 V. In case of colorimetric visualization, staining was performed with Coomassie brilliant blue R-250.

For immunodetection of the ThaADH-streptag fusion protein, the SuperSignal® West Femto kit (IBA GmbH, Goettingen, Germany) was applied, which is based on a streptactin-horse radish peroxidase conjugate. Protein transfer from the SDS-gel to a methanol activated PVDF membrane (Biotrace, Auckland, New Zealand) was performed in the XCell SurelockTM system (Life Technologies, Carlsbad, CA, USA) for 2 h at 30 V. The PVDF membrane was then washed three times with TBS-T buffer [20 $mmol \cdot L^{-1}$ Tris, 500 $mmol \cdot L^{-1}$ NaCl, 0.05% (v/v) Tween 20, pH 7.5] followed by the colorimetric assay, applying SuperSignal® Femto Maximum Sensitivity Substrate (Thermo Fisher Scientific, Waltham, MA, USA).

Enzyme Activity Assays

Assays for ADH activity were performed photometrically by measuring the consumption of the cofactor NADH. The standard assay was performed in 100 $mmol \cdot L^{-1}$ TEA buffer at a pH value of 6.4 with 3 $mmol \cdot L^{-1}$ substrate (1,2-cyclo-

hexanedione) and 250 μmol·L^{-1} NADH in 1 mL scale at 50 °C. The reaction was started by addition of ThaADH stock solution to a final concentration of 100 μg·mL^{-1}. Initial reaction rates were measured at a wavelength of 340 nm in 10 s intervals for 2 min. For determination of the pH optimum, acetate (pH 4.0, 5.0), phosphate (KP_i) (pH 6.0) and TEA buffer (pH 7.0, 8.0, 9.0) were utilized. For determination of the temperature optimum pH values were adjusted to 6.4 for each tested temperature.

For determination of the kinetic parameters of ThaADH, reaction conditions were modified. The enzyme concentration was reduced to 17 μg·mL^{-1} and the reaction time was increased to 10 min. Reactions were performed in 100 mmol·L^{-1} KP_i buffer (pH 6.0). For determination of the kinetic parameters of CPCR2 all reactions were performed under the same conditions in 100 mmol·L^{-1} TEA buffer (pH 7.33) and 25 °C. From activity assays performed at differing substrate concentrations, kinetic parameters were derived by non-linear regression. Activity data are shown in the Supporting Information (Tables S2–S8)

Product Identification

Identification of the reaction product of 1,2-cyclohexanedione reduction was performed on an Agilent 6890N Network Gas Chromatograph system with an Agilent HP 5973N Mass Selective Detector equipped with an Optima 35 MS column. A temperature program from 50–320 °C with a gradient of 10 °C min^{-1} was applied. The substrate was detected at 9.85 min (Supporting Information, Figures S2, S3, S5). The product 2-hydroxycyclohexanone was detected at 9.97 min (Sipporeting Informatipon, Figures S2 and S3).

Homology Modeling

Homology modeling of ThaADH structure was performed *via* the Swiss Model protein structure homology-modeling server (ProMod Version 3.70.).[38,39,40,41] The template search yielded several hits with sequence identities ranging between 25 and 30%. 25 models were generated applying the 25 best hits as template. The quality of the models was judged by the provided GMQE value. This value reflects the expected accuracy of the model taking into account the template structure as well as the model geometry and solvatation (QMean4).[33,34] To judge the local quality of the model, six residues (H78, P102, A103, D169, G316, Y322) in the active site were chosen and their local IDDT values were utilized. The IDDT value is a measure for the local expected similarity to the target.[33,34] Structural alignments and structure comparisons were performed with Yasara (version 12.10.3). The structural alignment and the superposition were conducted with build-in MUSTANG module.[42]

Acknowledgements

Deutsche Forschungsgemeinschaft (DFG) is greatly acknowledged for financial support within the research project AN 387/5-1 as well as the collaborative research network BioNoCo (GRK1166) for scientific support and software provision. Marco Boccola and Gaurao Dhoke from RWTH Aachen University are acknowledged for their kind support and fruitful discussions regarding molecular modeling. Prof. Gerold Barth and Sebastian Stark from TU Dresden are acknowledged for technical support in StrepTagII Immunodetection.

References

[1] B. Persson, J. Hedlund, H. Joernvall, *Cell. Mol. Life Sci.* **2008**, *65*, 3879–3894.
[2] H. Joernvall, B. Persson, J. Jeffrey, *Eur. J. Biochem.* **1987**, *167*, 195–201.
[3] E. Magonet, P. Hayen, D. Delforge, E. Delaive, J. Remacle, *Biochem. J.* **1992**, *287*, 361–365.
[4] J. Haberland, W. Hummel, T. Daussmann, A. Liese, *Org. Process Res. Dev.* **2002**, *6*, 458–462.
[5] M. Amidjojo, E. Franco-Lara, A. Nowak, H. Link, D. Weuster-Botz, *Appl Microbiol Biotechnol.* **2005**, *69*, 9–15.
[6] W. Kroutil, H. Mang, K. Edegger, K. Faber, *Curr. Opin. Chem. Bi*ol. **2004**, *8*, 120–126.
[7] A. Jakoblinnert, R. Mladenov, A. Paul, F. Sibilla, U. Schwaneberg, M. B. Ansorge-Schumacher, P. Dominguez de Maria, *Chem. Commun.* **2011**, *47*, 12230–12232.
[8] P. Hoyos, J. V. Sinisterra, F. Molinari, A. R. Alcantara, P. Dominguez de Maria, *Acc. Chem. Res.* **2010**, *43*, 288–299.
[9] J. Peters, T. Zelinski, T. Minuth, M. R. Kula, *Tetrahedron: Asymmetry* **1993**, *4*, 1683–1692.
[10] G. Gonzalo, I. Lavandera, K. Faber, W. Kroutil, *Org. Lett.* **2007**, *9*, 2163–2166.
[11] P. Schweiger, H. Gross, U. Deppenmeier, *Appl Microbiol Biotechnol.* **2010**, 87, 1415–1426.
[12] S. Leuchs, L. Greiner, *Chem. Biochem. Eng. Q.* **2011**, *25*, 267–281.
[13] V. Prelog, *Pure Appl. Chem.* **1964**, *9*, 119–130.
[14] J. B. Jones, I. Jakovac, *J. Chem.* **1982**, *60*, 19–28.
[15] J. Peters, T. Zelinski, T. Minuth, M. R. Kula, *Biocatalysis* **1993**, *8*, 31–46.
[16] J. Peters, T. Zelinski, T. Minuth, M. R. Kula, *Enzyme Microb. Technol.* **1993**, *15*, 950–958.
[17] J. Heidlas, R. Tressl, *Eur. J. Biochem.* **1990**, *188*, 165–174.
[18] T. Daussmann, H. G. Hennemann, European Patent EP 1763577 B, **2005**.
[19] J. C. Moore, D. J. Pollard, B. Kosjek, P. N. Devine, *Acc. Chem. Res.* **2007**, *40*, 1412–1419.
[20] B. Kosjek, J. Nti-Gyabaah, K. Telari, L. Dunne, J. C. Moore, *Org. Process Res. Dev.* **2008**, *12*, 584–588.
[21] W. Dangel, A. Tschech, G. Fuchs, *Arch. Microbiol.* **1989**, *152*, 273–279.
[22] M. Carmona, M. T. Zamarro, B. Blazquez, G. Durante-Rodriguez, J. F. Juarez, J. A. Valderrama, M. J. L. Barragan, J. L. Garcia, E. Diaz, *Microbiol. Mol. Biol. Rev.* **2009**, *73*, 71–130.
[23] D. A. Pelletier, C. S. Harwood, *J. Bacteriol.* **2000**, *182*, 2753–2760.
[24] D. Laempe, M. Jahn, G. Fuchs, *Eur. J. Biochem.* **1999**, *263*, 420–429.
[25] V. Hoellrigl, F. Hollmann, A. C. Kleeb, K. Buehler, A. Schmid, *Appl. Microbiol. Biotechnol.* **2008**, *81*, 263–273.

[26] A. Trincone, L. Lama, V. Lanzotti, B. Nicolaus, M. De Rosa, M. Rossi, A. Gambacorta, *Biotechnol. Bioeng.* **1990**, *35*, 559–564.
[27] A. S. Ramaswamy, M. El Ahmad, O. Danielsson, H. Joernvall, H. Eklund, *Protein Sci.* **1996**, *5*, 663–671.
[28] C. Ceccarelli, Z. X. Liang, M. Strickler, G. Prehna, B. M. Goldstein, J. P. Klinman, B. J. Bahnson, *Biochemistry* **2004**, *43*, 5266–5277.
[29] H. Man, C. Loderer, M. B. Ansorge-Schumacher, G. Grogan, *ChemCatChem* **2014**, *6*, 1103–1111.
[30] M. Karabec, A. Łyskowski, K. C. Tauber, G. Steinkellner, W. Kroutil, G. Grogan, K. Gruber, *Chem. Commun.* **2010**, *46*, 6314–6316.
[31] L. Esposito, F. Sica, C. A. Raia, A. Giordano, M. Rossi, L. Mazzarella, A. Zagari, *J. Mol. Biol.* **2002**, *318*, 463–477.
[32] S. Ramaswamy, M. Scholze, B. V. Plapp, *Biochemistry* **1997**, *36*, 3522–3527.
[33] P. Benkert, M. Kuenzli 1, T. Schwede, *Nucleic Acids Res.* **2009**, *37*, 510–514.
[34] P. Benkert, M. Biasini, T. Schwede, *Bioinformatics* **2011**, *27*, 343–350.
[35] A. Jakoblinnert, J. Wachtmeister, L. Schukur, A. V. Shivange, M. Bocola, M. B. Ansorge-Schumacher, U. Schwaneberg, *Protein Eng. Des. Sel.* **2013**, *26*, 291–298.
[36] S. Tabor, in: *Current Protocols in Molecular Biology*, (Eds.: F. M. Ausubel, R. Brent, R. E. Kingston, D. D. Moore, J. G. Seidman, J. A. Smith, K. Struhl), John Wiley & Sons, Inc., Hoboken, New Jersey, **1990**, pp 16.2.1–16.2.11.
[37] U. K. Laemmli, *Nature* **1970**, *227*, 680–685.
[38] M. Biasini, S. Bienert, A. Waterhouse, K. Arnold, G. Studer, T. Schmidt, F. Kiefer, T. G. Cassarino, M. Bertoni, L. Bordoli, T. Schwede, *Nucleic Acids Res.* **2014**, *42*, 252–258.
[39] K. Arnold, L. Bordoli, J. Koppl, T. Schwede, *Bioinformatics* **2006**, *22*, 195–201.
[40] N. Guex, M. C. Peitsch, T. Schwede, *Electrophoresis* **2009**, *30*, 162–173.
[41] F. Kiefer, K. Arnold, M. Kuenzli, L. Bordoli, T. Schwede, *Nucleic Acids Res.* **2009**, *37*, 387–392.
[42] A. S. Konagurthu, J. C. Whisstock, P. J. Stuckey, A. M. Lesk, *Proteins Struct. Funct. Bioinf.* **2006**, *64*, 559–574.

